

Communication

How to Increase the Analog-to-Digital Converter Speed in Optoelectronic Systems of the Seed Quality Rapid Analyzer

Sergey Sokolov ¹, Vladislav Kamenskij ² , Arthur Novikov ^{3,*}  and Vladan Ivetić ⁴

¹ Computer Technologies and Information Security Faculty, Rostov State University of Economics, 69, Bolshaya Sadovaya, Rostov-on-Don 344002, Russia; s.v.s.888@yandex.ru

² Management Information Technology Faculty, Rostov State Transport University, 2, Rostovskogo Strelkovogo Polka Narodnogo Opolcheniya sq., Rostov-on-Don 344038, Russia; kam-vladislav@yandex.ru

³ Mechanical Department, Voronezh State University of Forestry and Technologies named after G.F. Morozov, 8, Timiryazeva, Voronezh 394087, Russia

⁴ Faculty of Forestry, University of Belgrade, 1 Kneza Višeslava, 11030 Belgrade, Serbia; vladan.ivetic@sfb.bg.ac.rs

* Correspondence: arthur.novikov@vglta.vrn.ru; Tel.: +7-903-650-84-09

Received: 29 August 2019; Accepted: 30 September 2019; Published: 6 October 2019



Abstract: This invention is relevant when working as part of optoelectronic systems, including non-destructive quality control of forest seeds. The possibility of synthesis of the ultrafast optical analog-to-digital converter (ADC) providing conversion of analog information to digital in the sub-GHz range is considered. The functional scheme of the optical ADC, containing technologically well-developed optical elements is given; the principle of operation is described in detail. The possibility of increasing the speed of the ADC to make it potentially possible for optical data processing schemes is shown.

Keywords: forest seed rapid analyzer; optical analog-to-digital converter; optical bistable elements; optical waveguides; integrated optics

1. Introduction

In modern forest seed production, challenges for non-destructive seed quality control often arise [1]. Features of collection and storage of forest seeds suggest the presence of mobile Express analyzers [2]. They operate in different optical ranges, are designed on a modular basis and have the ability not only to diagnose, but also to separate [3,4] seeds by spectrometric properties [5–7]. The bases of these devices are optoelectronic systems [8] allowing, depending on the specific optical index of the seed, to calculate its viability [9–15]. The speed of any information-computing system depends to a significant extent on the speed of its interface, especially in a situation where it is used to control physical and technical processes in real time [16].

In this case, of particular importance is the speed of buffer devices that convert analog information into digital. For multi-bit converters (with the number of bits $N > 10$), the problem of speed information processing in the sub-GHz (and larger) range has not yet been solved. The lack of a high-speed interface negates all the advantages of any converter. To date, a very urgent task is the development of an analog-to-digital converter (ADC) with a conversion rate commensurate with the potential possible speeds of optical switching circuits.

Currently known ADCs:

- based on the use of electronic functional elements [17],

- ADC-based waveguide modulators of the type Mach-Zehnder [18],
- ADC based on the use of optical bistable elements (OBEs) and distributed optical waveguides [19], etc.

The obvious disadvantages of electronic ADCs are their low speeds, which decrease even more with the growth of the ADC bit rate, and high complexity. In turn, the disadvantages of the ADC based on waveguide Mach-Zehnder type modulators [18] are the ability to convert the input analog signal only to gray code (and not the positional binary code) and the overall low performance of the ADC due to the need to use a large number of electronic elements (photodetectors, amplifiers, comparator, etc.) in the terminal cascade with a total response time $\geq 10^{-6}$ s. Such a short response time does not allow to process information in the sub-GHz range.

Among the listed ADC, the fastest is the ADC based on waveguide optical elements [19], but in this ADC the conversion time is directly proportional to its output code and the pulse repetition period. Since this ADC operates in a cyclic mode (at the end of the conversion time interval, the counter is set to the initial state and therefore the conversion always starts from zero), its disadvantage is that it does not have a very high speed, which does not allow analog-to-digital conversion in the sub-GHz range.

Let us consider further the possibility of synthesis of optical ADC, which provides conversion into positional binary code of electrical analog signals in control and communication systems, information processing in which is carried out in sub-GHz and large ranges.

2. The Optical ADC Principle

The functional scheme of the considered optical ADC, focused on the possibility of integrated optical performance [18,20], is shown in Figure 1.

N-bit optical ADC contains a coherent radiation source 1, K -output optical splitter 2 ($K = M + 1$, $M = 2^N - 1$, N —number of ADC discharges), M optical transparencies 3_i ($i = 1 \dots M$), M optical Y-unifiers 4_i , two groups of M OBEs in each 5_i and 5_{M+i} , electro-optical amplitude modulator 6, optical phase modulator 7, M -output optical splitter 8, M N -output optical splitters 9_i , N M -input optical unifiers 10_j , and N photodetectors 11_j ($j = 1 \dots N$).

It should be noted that a significant number of optical splitters that are part of this ADC lead to strict requirements for their manufacturing, providing a maximum relative error of signal transmission, which in assessing the accuracy of the ADC can be neglected, of no more than 0.001%. To date, a similar level of technology for the production of optical splitters has been achieved by Michael S. Cohen (Qikertown, PA, USA) and Nanonics Imaging Ltd. (Jerusalem, Israel); splitters that have insertion loss less than 0.1 dB, flatness ratio offshoots 0.1 dB, back reflection less than -60 dB. When using optical splitters with less qualitative characteristics, correction of signal distortions can be carried out, for example, due to a corresponding change in the transmission coefficients of optical transparencies 3_i (see Figure 1).

OBEs 5_i ($i = 1 \dots 2M$) are optical elements that transmit an optical signal from the input to the first (direct) output, if the amplitude of the input optical signal is greater than or equal to the specified threshold value. Otherwise, the optical signal is transmitted to the second (inverse) output. OBEs may be made in the form of optical transistors [20], optically connected waveguides [18,20,21] and others [22,23].

The OBE threshold of the first group 5_i ($i = 1 \dots M$) is equal to $N - 1/2M$ conventional units, and the threshold of OBEs of the second group 5_{M+i} is equal to $N + 1/2M$ conventional units. The light-absorbing outputs are the second (inverse) OBEs outputs of the first group, 5_i , and the first (direct) OBEs outputs of the second group, 5_{M+i} . The input of the optical ADC U is the control input of electro-optical amplitude modulator 6.

The scheme of connection of the functional elements of the optical ADC is shown in Figure 1; it should be noted that the outputs from the first to the M -th K -output optical splitter 2 are connected to the inputs of optical banners $3_1 \dots 3_M$, and $(M + 1)$ -th. The output of optical splitter 2 is connected to the information input of electro-optical amplitude modulator 6.

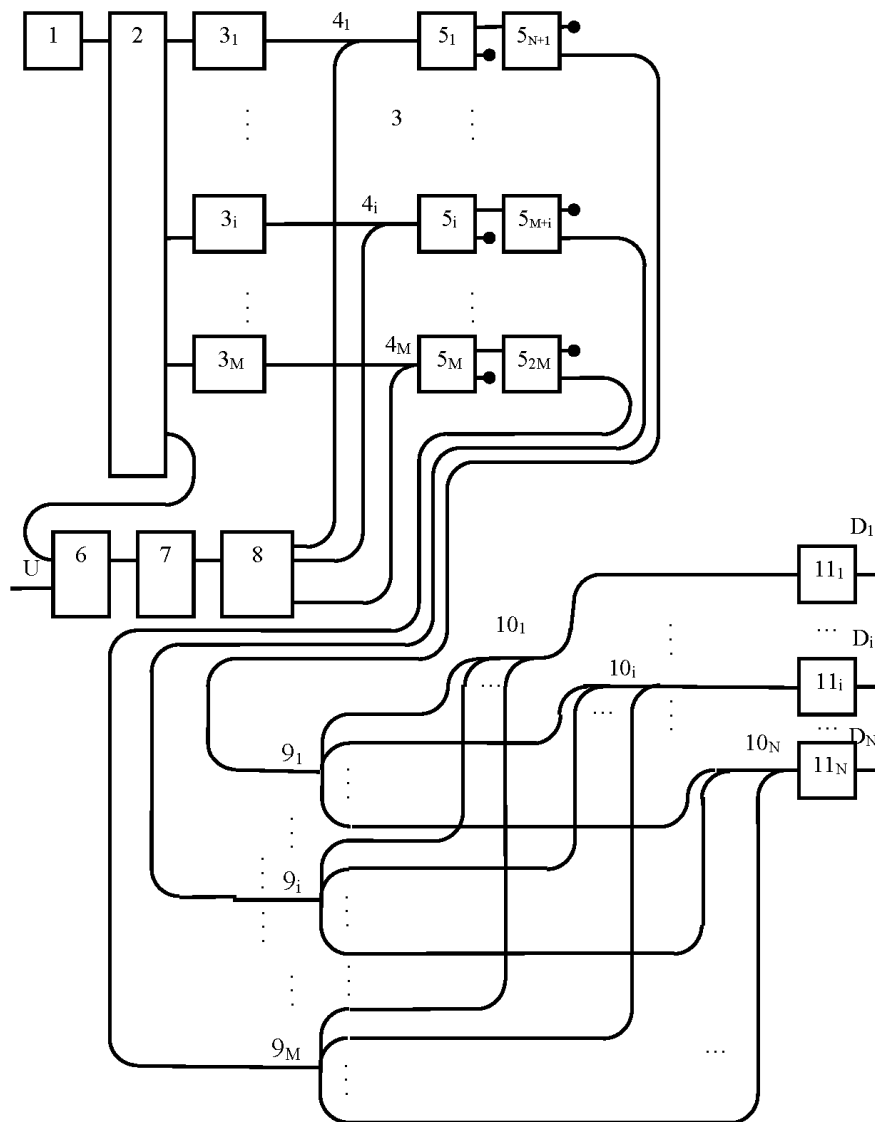


Figure 1. Function diagram of the analog-to-digital converter.

A feature of the optical scheme of this ADC is also that the outputs of N -output optical splitters 9_i are connected to the inputs of M -input optical unifiers 10_j ($j = 1 \dots N$) in such a way that in the presence of an optical signal at the input of i -th N -output optical splitter 9_i , a positional binary code of the number “ i ” is formed at all N outputs of M -input optical splitters 10_j . At the same time, some optical branching of N -output optical splitters 9_i are light-absorbing or do not absorb light waves. This process is explained by the presence/absence of appropriate connections between the optical splits of N -output optical splitters 9_i and the optical branches of M -input optical splitters 10_j . The outputs of the M -input optical unifiers 10_j are already optically connected to the inputs of the same-name photodetectors 11_j , the outputs of which “ $D_1 \dots D_N$ ” are the outputs of the ADC.

Each optical splitter 9_i has a number of outputs (branches) equal to the number of ones in a binary code at number “ i ”, and these outputs through the corresponding combiner 10_j are connected to the inputs of sensors 11_j , each of which corresponds to the same category of “ D_j ” of the output binary code. Thus, when an optical signal arrives at the input of splitter 9_i at the ADC outputs, “1”s are formed at those positions of the binary code that correspond to the number “ i ” (“0”—at the rest).

The optical signal with the amplitude $M \cdot K$ conventional units from the output of the coherent radiation source 1 enters the input of the K -output optical splitter 2. Due to the branching of the optical flow, K -output optical splitter 2 at each output generated optical signal with an amplitude

of M conventional units, providing the amplitude of the optical signal at the output of the optical transparency $3i$ transfer ratio $(N + i/M)/M$ is equal to $N + i/M$ unit.

The optical signal from the K -th output of the K -output optical splitter 2 is fed to the information input of the electro-optical amplitude modulator 6. If the input of the device and, consequently, at the control input of the electro-optical amplitude modulator 6 is input signal U_{IN} , the output of the electro-optical amplitude modulator 6 is formed an optical signal with the amplitude $U \bullet M$ conventional units, where $U = U_{IN}/U_{max}$ ($U < 1$), U_{IN} is the current input voltage, U_{MAX} is the maximum input voltage ($U_{MAX} = M$ conventional unit).

From the output of the electro-optical amplitude modulator 6, the optical signal enters the input of the optical phase modulator 7. After passing the optical phase modulator 7, the optical signal changes the phase to π and enters the M -output optical splitter 8. After passing the M -output optical splitter 8, the optical signal decreases in amplitude by a factor of M and enters the second inputs of M optical Y-connectors $4i$ ($i = 1 \dots M$) with amplitude U conventional units.

Since the addition of two coherent antiphase optical signals subtracts their amplitudes, the output of the first optical Y-unifier 4_1 signal amplitude will be: $(N + 1/M) - U$ conventional units, at the output of the second optical Y-unifier 4_2 , respectively: $(N + 2/M) - U$ conventional units. At the output of the i -th optical Y-unifier $4i$, the signal amplitude will be equal to $(N + i/M) - U$ conventional units.

In order for the optical signal to pass from the output of the optical Y-unifier 4_i through both OBEs: $5i$ and 5_{M+i} , its amplitude must be greater than the threshold of operation of OBEs $5i$ and less than the threshold of operation of OBEs 5_{M+i} . At any U , this condition will be met only for one pair of OBEs $5i$ and 5_{M+i} and accordingly only one input of N -output optical splitter 9_i will receive an optical signal.

Thus, at $U = 1/M$, the amplitude of the optical signal from the output of the first optical Y-unifier 4_1 is greater than the threshold of operation of OBEs 5_1 : $(N + 1/M) - U = N > N - 1/2M$ conventional units, therefore, the optical signal with the amplitude of the N conventional units will be held at the first output, and then fed to the input of OBEs 5_{M+1} . Since the amplitude of the optical signal at the input OBEs 5_{M+1} is less than the threshold of its operation $N < N + 1/2M$ conventional units, the optical signal will pass to its second output and then to the input of the N -output optical splitter 9_1 .

The amplitude of the optical signal from the output of the second optical Y-unifier 4_2 is greater than the threshold of operation of OBEs 5_2 : $(N + 2/M) - U = N + 1/M > N - 1/2M$ conventional units, so the optical signal will pass to its first output and will go to the input of OBEs 5_{M+2} . Since the amplitude of the optical signal at the input OBEs 5_{M+2} is greater than the threshold of its operation $N + 1 > N + 1/2M$ conventional units, the optical signal will pass to its first output, which is absorbing.

The amplitude of the optical signal from the output of the optical Y-unifier 4_M is greater than the threshold of operation of OBEs 5_M : $N + (M - 1)/M > N - 1/2M$ conventional units, so the optical signal will pass to its first output and go to the input of OBEs 5_{2M} . Since the amplitude of the optical signal at the input of the OBEs 5_{2M} is also greater than the threshold of its operation $N + N - 1 > N + 1/2M$ conventional units, the optical signal will pass to its first output, which is absorbing.

Thus, at $U = 1/M$ at the input of the device, the optical signal will be only at the input of the N -output optical splitter 9_1 .

At $U = i/M$, the amplitude of the optical signal from the output of the i -th optical Y-unifier 4_i is greater than the threshold of operation of OBEs 5_i : $(N + i/M) - U = N > N - 1/2M$ conventional units, therefore the optical signal with the amplitude of the N conventional units will be held at the first exit, and then fed to the input of OBEs 5_{M+i} . Since the amplitude of the optical signal at the input of OBEs 5_{M+i} is less than the threshold of its operation $N < N + 1/2M$ conventional units, the optical signal will pass to its second output and then to the input of the N -output optical splitter 9_i .

The amplitude of the optical signal from the output $(i-1)$ -th of the optical Y-unifier 4_{i-1} is less than the threshold of operation of OBEs 5_{i-1} : $(N + (i - 1)/M) - U = N - 1/M < N - 1/2M$ conventional unit. The optical signal will therefore pass to its second output, which is the absorbing.

The amplitude of the optical signal from the output $(i + 1)$ -th of the optical Y-unifier 4_{i+1} is greater than the threshold of operation of OBEs 5_{i+1} : $(N + (i + 1)/M) - U = N + 1/M > N - 1/2M$ conventional

unit, so the optical signal will pass to its first output and will go to the input of OBEs 5_{M+i+1} . Since the amplitude of the optical signal at the input OBEs 5_{M+i+1} is greater than its threshold $N + 1/M > N + 1/2M$ conventional unit, the optical signal will pass to its first output, which is absorbing.

Thus, at $U = i/M$ at the input of the device, the optical signal will be only at the input of the N -output optical splitter 9_i .

Since only those outputs of N -output optical splitters $9_1 \dots 9_M$ are connected to the inputs of M -input optical unifiers $10_1 \dots 10_N$, which allow to form a binary code of the number “ i ”, as a result, optical signals will appear only on the outputs of M -input optical unifiers $10_1 \dots 10_N$ corresponding to the position binary code of the number “ i ”. The optical signals from the outputs of the M -input optical unifiers $10_1 \dots 10_N$ are then fed to the inputs of the photodetectors $11_1 \dots 11_N$, forming a positional binary code $\{D_1 \dots D_N\}$ at the output of the ADC. This code is a binary analogue of the input signal U .

3. Conclusions

When analog voltage U is applied to the input of the device, a corresponding positional binary code is formed at the output of the device. The speed of this ADC is determined mainly by the response time of the electro-optical amplitude modulator (5–10 ns) and photo detectors (100 ps), which allows the conversion of signals with frequency up to 2×10^8 Hz. This speed completely satisfies the requirements for signal conversion in rapid seed analyzers, where the ADC is used as one of the main functional blocks [2–4].

Moreover, if the output signals of this ADC are further used not in electronic, but in optical circuits for computing and processing information [23–26], then the output photo detectors $11_1 \dots 11_N$ can be excluded from the conversion process, which will lead to an increase in the speed of the ADC to potentially possible for optical information processing circuits.

Author Contributions: Conceptualization, S.S., A.N. and V.I.; methodology, S.S. and V.K.; formal analysis, S.S. and V.K.; investigation, S.S. and A.N.; writing—original draft preparation S.S., V.K., A.N. and V.I.; writing—review and editing, S.S., A.N. and V.I.; supervision, S.S.

Funding: This research received no external funding.

Conflicts of Interest: The authors declare no conflict of interest.

References

1. Novikov, A.I.; Novikova, T.P. Non-destructive quality control of forest seeds in globalization: Problems and prospects of output innovative products. In Proceedings of the Globalization and Its Socio-Economic Consequences, Zilina, Slovakia, 10–11 October 2018; University of Zilina: Rajcke Teplice, Slovakia, 2018; pp. 1260–1267.
2. Albekov, A.U.; Drapalyuk, M.V.; Morkovina, S.S.; Vovchenko, N.G.; Novikov, A.I.; Sokolov, S.V.; Novikova, T.P. Express Analyzer of Seed Quality. RU Patent 2675056, 14 December 2018.
3. Albekov, A.U.; Drapalyuk, M.V.; Morkovina, S.S.; Vovchenko, N.G.; Novikov, A.I.; Sokolov, S.V.; Novikova, T.P. Device for Seeds Sorting. RU Patent 2682854, 21 March 2019.
4. Albekov, A.U.; Drapalyuk, M.V.; Morkovina, S.S.; Novikov, A.I.; Vovchenko, N.G.; Sokolov, S.V.; Novikova, T.P. Seed Sorting Device. RU Patent 2687509, 14 May 2019.
5. Novikov, A.I. Visible wave spectrometric features of scots pine seeds: The basis for designing a rapid analyzer. *IOP Conf. Ser. Earth Environ. Sci.* **2019**, *226*, 012064. [[CrossRef](#)]
6. Novikov, A.I.; Saushkin, V.V. Infrared range spectroscopy: The study of the pine seed coat parameters. *For. Eng. J.* **2018**, *8*, 30–37. (In Russian)
7. Novikov, A.I.; Ivetić, V.; Drapalyuk, M.V.; Sokolov, S.V. VIS-NIR wave spectrometric features of acorns (*Quercus robur* L.) for machine grading. *IOP Conf. Ser. Earth Environ. Sci.* (under review).
8. Sokolov, S.V.; Novikov, A.I. New optoelectronic systems of seeds rapid analysis in forestry production. *For. Eng. J.* **2019**, *9*, 5–13. (In Russian)

9. Mukasa, P.; Wakholi, C.; Mo, C.; Oh, M.; Joo, H.-J.; Kwon Suh, H.; Cho, B.-K. Determination of viability of retinispora (hinoki cypress) seeds using FT-NIR spectroscopy. *Infrared Phys. Technol.* **2019**, *78*, 62–68. [[CrossRef](#)]
10. Schelin, M.; Tigabu, M.; Eriksson, I.; Sawadogo, L.; Christer Odén, P. Predispersal seed predation in *Acacia macrostachya*, its impact on seed viability, and germination responses to scarification and dry heat treatments. *New For.* **2004**, *27*, 251–267. [[CrossRef](#)]
11. Xia, Y.; Xu, Y.; Li, J.; Zhang, C.; Fan, S. Recent advances in emerging techniques for non-destructive detection of seed viability: A review. *Artif. Intell. Agric.* **2019**, *1*, 35–47. [[CrossRef](#)]
12. Ambrose, A.; Lohumi, S.; Lee, W.-H.; Cho, B.K. Comparative nondestructive measurement of corn seed viability using Fourier transform near-infrared (FT-NIR) and Raman spectroscopy. *Sens. Actuators B Chem.* **2016**, *224*, 500–506. [[CrossRef](#)]
13. Clark, R.L.; McFarland, H.A. Studies of the optical-properties of cottonseed as related to seed viability 1. *Trans. ASAE* **1979**, *22*, 1178–1180. [[CrossRef](#)]
14. Novikov, A.I. Forest seeds rapid analysis: The choice of the effective quality indicator. In Proceedings of the Proceeding in Ecological and Biological Bases of Increasing Productivity and Sustainability of Natural and Artificially Renewed Forest Ecosystems, Voronezh, Russia, 4–6 October 2018; Voronezh State University of Forestry and Technologies named after G.F. Morozov: Voronezh, Russia, 2018; pp. 559–567.
15. Tigabu, M.; Daneshvar, A.; Jingjing, R.; Wu, P.; Ma, X.; Odén, P.C. Multivariate Discriminant Analysis of Single Seed Near Infrared Spectra for Sorting Dead-Filled and Viable Seeds of Three Pine Species: Does One Model Fit All Species? *Forests* **2019**, *10*, 469. [[CrossRef](#)]
16. Sokolov, S.V.; Kamenskij, V. Optical spatial-frequency analog-digital converter. *J. Instrum. Eng.* **2013**, *56*, 35–38. (In Russian)
17. Tietze, U.; Schenk, K. *Semiconductor Circuitry*; DMK Press: Moscow, Russia, 2008. (In Russian)
18. Semenov, A.S.; Smirnov, V.L.; Shmalko, A.V. *Integrated Optics for Information Transmission and Processing Systems*; Radio and Communication: Moscow, Russia, 1990. (In Russian)
19. Sokolov, S.V.; Shcherban, I.V.; Cibrienko, V.V. Optical Analog-to-Digital Converter. RU Patent 2177165, 24 May 2000.
20. Akaev, A.A.; Maiorov, S.A. *Optical Methods of Information Processing*; High School: Moscow, Russia, 1988. (In Russian)
21. Athale, R.A.; Collins, W.C. Optical matrix–matrix multiplier based on outer product decomposition. *Appl. Opt.* **1982**, *21*, 2089–2090. [[CrossRef](#)] [[PubMed](#)]
22. Bai, J.; Chandraker, M.; Ng, T.-T.; Ramamoorthi, R. A dual theory of inverse and forward light transport. Computer Vision—ECCV 2010. Lecture Notes in Computer Science. In Proceedings of the European Conference on Computer Vision, Heraklion, Crete, Greece, 5–11 September 2010; Daniilidis, K., Maragos, P., Paragios, N., Eds.; Springer: Berlin/Heidelberg, Germany, 2010; Volume 6312, pp. 294–307.
23. Guilfoyle, P.S.; Stone, R.V.; Zeise, F.F. Digital Optical Interconnects for Photonic Computing. Available online: <https://doi.org/10.1117/12.174532> (accessed on 2 May 1994).
24. Goodman, J.W. *Introduction to Fourier Optics*; Roberts and Company Publishers: Englewood, CO, USA, 2005.
25. Leith, E.N. The evolution of information optics. *IEEE J. Sel. Top. Quantum Electron.* **2000**, *6*, 1297–1304. [[CrossRef](#)]
26. Psaltis, D.; Athale, R.A. High accuracy computation with linear analog optical systems: A critical study. *Appl. Opt.* **1986**, *25*, 3071–3077. [[CrossRef](#)] [[PubMed](#)]

